

Building an Anti-Tip System for Robots Transporting People Up and Down the Stairs

Duong Tan Dat

Faculty of Mechanical Engineering, Vinh Long University of Technology Education, Vietnam
datdt@vlute.edu.vn

Le Hong Ky

Faculty of Mechanical Engineering, Vinh Long University of Technology Education, Vietnam
kylh@vlute.edu.vn (corresponding author)

Son Hoang

Faculty of Electronics Engineering 1, Posts and Telecommunications Institute of Technology, Vietnam
hoangson@ptit.edu.vn

Tran Duc Thuan

Faculty of Mechanical Engineering, Vinh Long University of Technology Education, Vietnam
thuandauto@yahoo.com

Received: 18 February 2025 | Revised: 24 March 2025, 6 April 2025, and 10 April 2025 | Accepted: 12 April 2025

Licensed under a CC-BY 4.0 license | Copyright (c) by the authors | DOI: <https://doi.org/10.48084/etasr.10618>

ABSTRACT

This paper presents an anti-roll control model for a human transport robot that can go up and down stairs with different slopes. The anti-roll control system is implemented by the process of controlling the robot's center of gravity and the adaptive mechanism. The anti-roll equation when moving up and down stairs is proposed with a balance system by a linear actuator to help control the balance and anti-roll according to the slope of the stairs. The phenomenon of oscillation and overturning towards the moving direction at the last step of the stairs is also considered and analyzed, and a control equation is built to limit this phenomenon. The suitability of the dynamic equations is verified through simulation results on Matlab Simulink software. The experimental model was constructed and tested in real conditions with a slope of 35°. The experimental results of the human transport robot show that the robot is balanced and stable when moving up and down stairs. This shows the effectiveness of the anti-roll model for the crawler human transport robot.

Keywords-human transport robot; balance control; vibration reduction; anti-overturn

I. INTRODUCTION

Currently, the development of high-rise buildings, public staircases, or urban structures with steep slopes, etc. has brought many obstacles to people with lower limb disabilities, although electric wheelchairs have been researched and equipped for them all over the world. Electric wheelchairs operate effectively with a weight of 50-70 kg and can move at a speed of 35°, a distance of 20 km/h [1]. However, electric wheelchairs are mainly used for moving on flat surfaces. Besides, many studies have been conducted on improving electric wheelchairs into robots capable of overcoming obstacles, especially the function of going up and down stairs using a moving mechanism with a round wheel cluster, a crawler, a high step, or a hybrid mechanism [2, 3]. Initial studies on building dynamic equations and experimentally verifying the ability of robots to move on flat surfaces and on

stairs with crawlers have also been carried out [4, 5]. Nonetheless, the challenge of developing a control system for balance, anti-overturning, adaptability, and user safety remains unresolved. Authors in [6] and [7] have studied and analyzed the model and operating state of robots when going up and down stairs, considering the risk of overturning due to the deviation of the center of gravity. However, the robot still has the problem of tipping over, the robot's movement process always requires support from behind, and the robot's operation is limited by the size of the stairs [7]. In the study in [8], the robot operates to transport people up and down stairs with the user's back facing down, giving feasible results with the dynamic model built considering the robot's center of gravity position. However, the risk of the robot tipping over has not been completely overcome in this study. In the studies, most of the robot's dynamic equations are based on the center of gravity projection method to analyze its stability in static mode. The

equations consider the seat and the direction of movement of the robot when going up the stairs according to the user's view [9]. Authors in [10] performed semi-automatic tracking based on system dynamics to facilitate automatic posture adjustment according to the terrain. The overturning restriction through a logic control system between components has been performed on a robot system with a moving system using a wheel cluster combined with a crawler, which is studied based on analyzing the built dynamic equations [11, 12]. Authors in [13] reviewed and surveyed the closed-loop control system based on the kinematic and dynamic equations of the robot to control the deviations and maintain stability during the movement of the robot. The robot system consists of three moving crawler segments that work together to help the robot move up the stairs, and the control algorithm is also applied to this type of robot system [14]. The results of the analysis of the operation of the wheel cluster robot combined with the crawler mechanism are analyzed and the system's operating ability is evaluated with the ability to move up the stairs, but the anti-overturn control system is still limited [15]. Authors in [16] investigate an experimental crawler robot that can transport people upstairs with a slope of 30° and a step height of not more than 20 cm. The system uses a PID controller with a chair balance structure, however, the system response is slow. In general, the above studies have used kinematic and dynamic models of robot systems to test the ability of robots to move on stairs, and some studies have built anti-overturn models. However, the limitations of balance, overturning, oscillation, stability, and the inability of robot structures to operate in different environments still exist. A robot structure with an anti-overturn system, balance, environmental adaptation, and effective operation under all impact conditions is necessary to be solved simultaneously. Robot control systems need to be adaptive and respond promptly to environmental changes. Authors in [17] used fuzzy controllers in the adaptive control during robot operation [17]. However, the control system depends on experience. Sliding controllers are evaluated to have many advantages with high stability, fast response, and durability to disturbances. However, chattering occurs [18]. Furthermore, sliding control algorithms with PID sliding surfaces are effective in limiting the chattering phenomenon of the controller [19].

This study will establish an anti-roll system for robots when transporting people up and down stairs by applying the Lagrange control theory [20]. The study will develop dynamic equations to prevent rolling for robots transporting people, which can automatically balance, adapt, reduce vibration, and stabilize through linear actuators. The limitations of rolling and vibration of the robot are also considered during the process of the robot moving up and down stairs.

II. HUMAN TRANSPORT ROBOT STRUCTURE

The human transport robot operates in two separate modes, moving on flat surfaces with round wheeling and moving on stairs with crawlers. The robot's anti-overturn system features a balancing mechanism and an adaptive mechanism, as illustrated in Figure 1.

The automatic seat position balancing system controls the robot's center of gravity, performing anti-overturn for the robot

when moving on stairs. The automatic adaptation mechanism reduces oscillation and anti-overturn when the robot changes state upon reaching the last step of the stairs. The robot ascends or descends stairs while carrying people, always moving from top to bottom. The balancing mechanism adjusts the seat's center of gravity to align with the slope of the stairs. Under normal operating conditions, the robot always contacts at least two steps, and the seat plane is controlled to ensure it is parallel to the flat plane, so it almost does not overturn. This adjustment helps to maintain the stability of the robot on many different slopes. The phenomenon of vibration at the last step of the stairs is limited by the adaptation mechanism. The mechanism helps the robot to make smooth contact with the surface of the stair platform to limit the vibration for the robot. The human transport robot is stabilized, balanced, and anti-overturned during the movement, which is performed on the basis of dynamic equations built during the robot's movement.

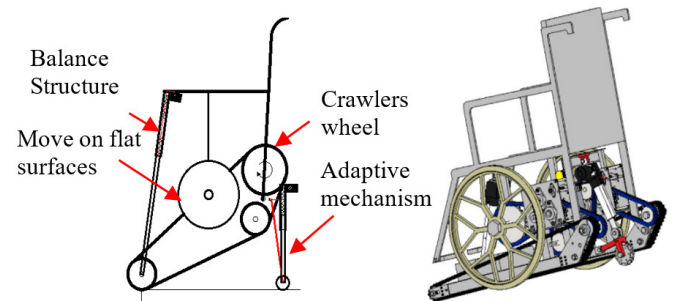


Fig. 1. Structural diagram and 3D model of the human transport robot.

III. ANTI-TIP CONTROL EQUATION FOR MAN-TRANSPORT ROBOTS

A. Control Equation for Robot Balancing on Stairs

Balance control during the process of robot transporting people up and down stairs is an important and indispensable stage in robot anti-overturn control. The robot moves on the stairs without overturning when the seat position is controlled parallel to the flat surface. The condition of the robot as it moves without tipping over is illustrated in Figure 2. In which, θ ($^\circ$) is the slope of the robot when moving, and the balance system will adjust the center of gravity of the seat as a counterweight to prevent the robot from overturning.

In the coordinate system depicted in Figure 2, $G_R(l_{Rx}, l_{Ry})$ is the center of gravity of the robot frame and $G_n(l_{nx}, l_{ny})$ is the center of gravity of the human transport mechanism. When the robot moves on the plane shown in Figure 2(a), the coordinate system is defined as follows:

$$\begin{cases} l_{Rx} = L \cos \beta \\ l_{Ry} = L \sin \beta \end{cases} \Rightarrow \begin{cases} \dot{l}_{Rx} = -L \sin \beta \\ \dot{l}_{Ry} = L \cos \beta \end{cases} \quad (1)$$

$$\begin{cases} l_{nx} = a_2 - b \cos \alpha_0 \\ l_{ny} = C + b \sin \alpha_0 \end{cases} \Rightarrow \begin{cases} \dot{l}_{nx} = -b \dot{\alpha}_0 \sin \alpha_0 \\ \dot{l}_{ny} = b \dot{\alpha}_0 \cos \alpha_0 \end{cases} \quad (2)$$

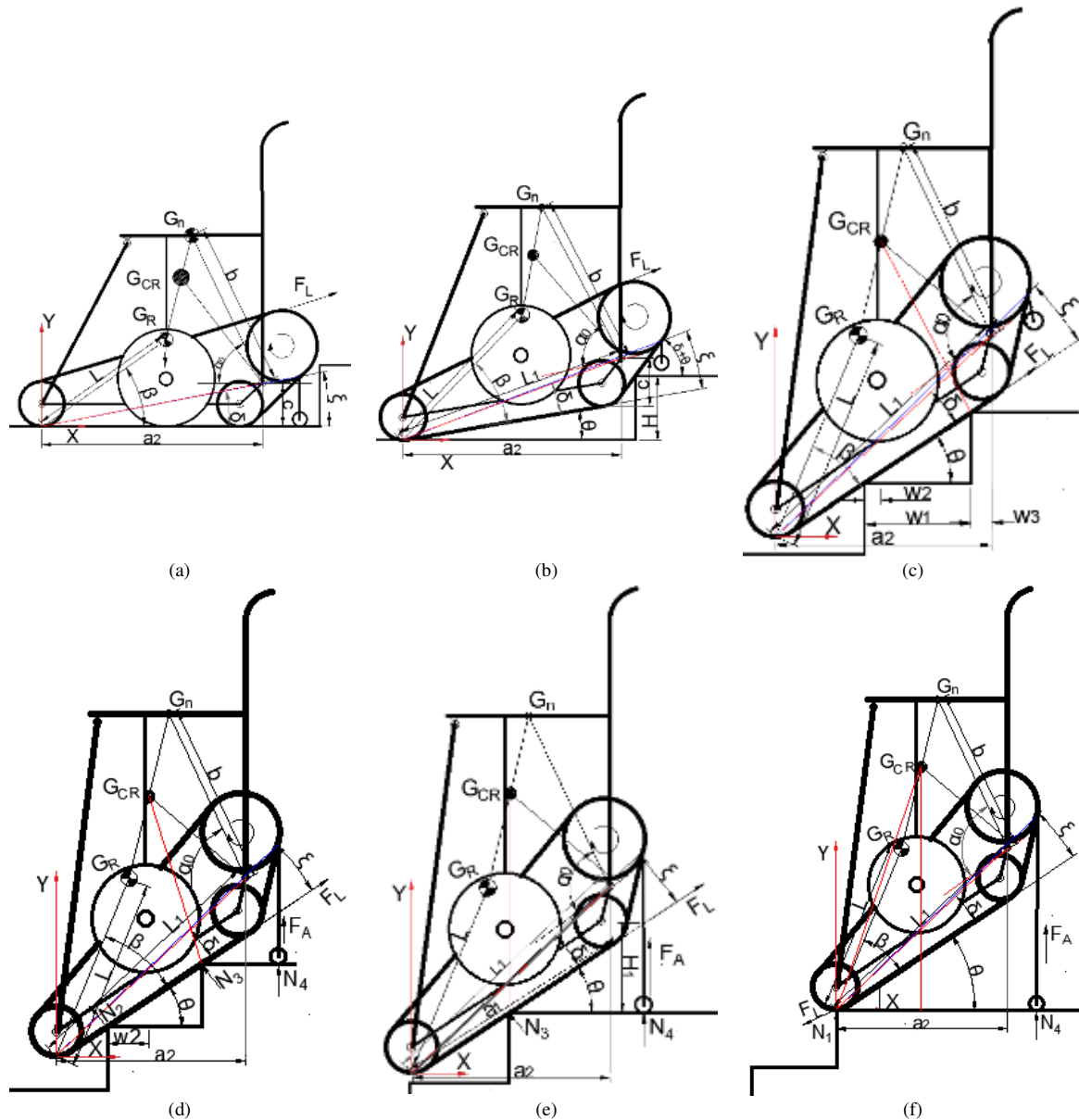


Fig. 2. State diagram of the stair-climbing robot.

When the robot moves on steps with a slope of θ , the center of gravity coordinate system is set as shown in Figure 2(b), and the center of gravity position equation is given in (3) and (4):

$$\begin{cases} l_{Rx} = L \cos(\beta + \theta) \\ l_{Ry} = L \sin(\beta + \theta) \end{cases} \Rightarrow \begin{cases} \dot{l}_{Rx} = -L\dot{\theta} \sin(\beta + \theta) \\ \dot{l}_{Ry} = L\dot{\theta} \cos(\beta + \theta) \end{cases} \quad (3)$$

$$\begin{cases} l_{nx} = L_1 \cos(\theta + \delta) - b \cos(\alpha_0) \\ l_{ny} = L_1 \sin(\theta + \delta) + b \sin(\alpha_0) \end{cases} \Rightarrow \begin{cases} \dot{l}_{nx} = -L_1 \dot{\theta} \sin(\theta + \delta) + b \dot{\alpha}_0 \sin(\alpha_0) \\ \dot{l}_{ny} = L_1 \dot{\theta} \cos(\theta + \delta) + b \dot{\alpha}_0 \cos(\alpha_0) \end{cases} \quad (4)$$

The robot's center of gravity $G_{CR}(l_{cx}, l_{cy})$ is adjusted based on changes in the robot's tilt angle (Figures 2(b), 2(c), 2(d), 2(e), and 2(f)):

$$l_{cx} = \frac{m_n l_{nx} + m_R l_{Rx}}{m_e}; l_{cy} = \frac{m_n l_{ny} + m_{Ry}}{m_e} \quad (5)$$

In the equations, L_1 (mm) denotes the distance from the robot frame's center of gravity to the coordinate angle, L (mm) signifies the distance from the adaptive mechanism to the passive wheel, β ($^\circ$) represents the angle of the robot frame's center of gravity, b (mm) indicates the distance from the chair's rotation axis to the chair's center of gravity, C (mm) is the distance from the rotation axis to the chain surface, α_0 ($^\circ$) is

the rotation angle of the initial chair center, ξ ($^\circ$) is the angle between the adaptive mechanism and the chain surface, δ ($^\circ$) is the angle between the chair's rotation axis and the chain surface, a_2 (mm) is the distance from the passive wheel to the chair's rotation axis, m_R , m_n (kg) are the robot frame's mass and the user's mass, respectively, and m_e (kg) is the total mass of the robot.

The robot moves on stairs with a change in slope θ . If there is an overturning phenomenon, it is due to the unbalanced center of gravity G_{CR} . To overcome this, a linear actuator is set to control the center of gravity according to the change in the tilt angle θ measured from the IMU sensor. Then, the robot center of gravity coordinate system is controlled based on the coordinate values of the seat G_n and the robot frame coordinates G_R , the position, and the coordinate system, as shown in Figure 3.

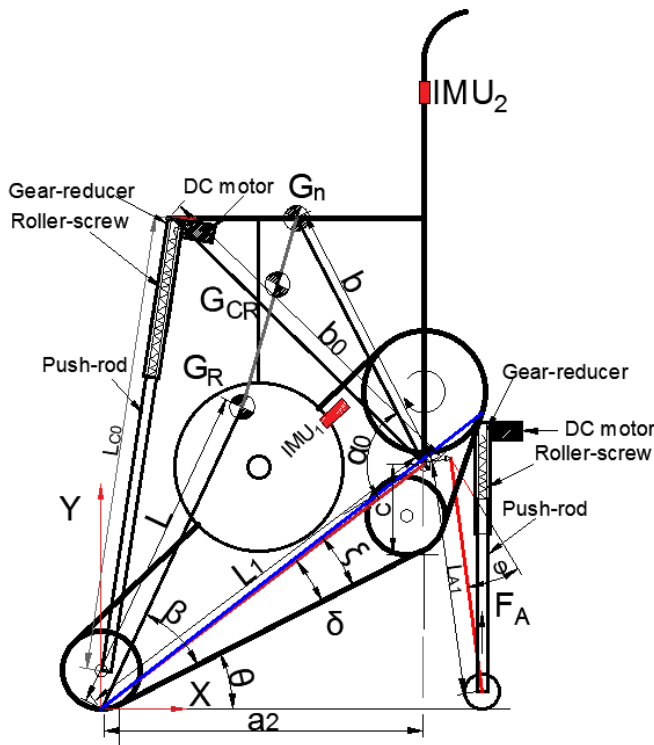


Fig. 3. Balance control diagram for stair-climbing robot.

The kinetic energy and the potential energy of the robot always change during the movement (Figure 2). The optimal control theory, as proposed by Lagrange [17] is used to develop the control equation for the robot's anti-overturn balance. Considering the kinetic energy equation T (J) of the robot operating on stairs with a slope of θ in the form:

$$\sum T = T_R + T_n = \frac{1}{2} m_R v_R^2 + \frac{1}{2} m_n v_n^2 \quad (6)$$

$$\begin{cases} v_R^2 = \dot{i}_{R_x}^2 + \dot{i}_{R_y}^2 = L^2 \dot{\theta}^2 \\ v_n^2 = \dot{i}_{n_x}^2 + \dot{i}_{n_y}^2 = L_1^2 \dot{\theta}^2 + b^2 \dot{\alpha}_0^2 + 2L_1 b \dot{\theta} \dot{\alpha}_0 \cos(\alpha_0 + \theta + \delta) \end{cases} \quad (7)$$

where v_R (m/s) is the displacement velocity of the robot and v_n (m/s) is the displacement velocity of the seat. Substituting (7) into (6), the formula is as follows:

$$\sum T = \frac{1}{2} m_R L^2 \dot{\theta}^2 + \frac{1}{2} m_n \left(L_1^2 \dot{\theta}^2 + b^2 \dot{\alpha}_0^2 + 2L_1 b \dot{\theta} \dot{\alpha}_0 \cos(\alpha_0 + \theta + \delta) \right) \quad (8)$$

The total potential energy of the system is determined as follows:

$$\begin{aligned} \sum P &= P_n + P_R \\ &= m_R g L \sin(\beta + \theta) + m_n g (L_1 \sin(\theta + \delta) + b \sin(\alpha_0)) \end{aligned} \quad (9)$$

where P_n (J), P_R (J) are the potential energy at the center of gravity of the seat and the potential energy at the center of gravity of the robot. The Lagrangian equation of the system is of the form:

$$\begin{aligned} L_{CR} = \sum T - \sum P &= \frac{1}{2} m_R (L^2 \dot{\theta}^2 - 2g L \sin(\beta + \theta)) + \\ & \frac{1}{2} m_n \left[L_1^2 \dot{\theta}^2 + b^2 \dot{\alpha}_0^2 + 2L_1 b \dot{\theta} \dot{\alpha}_0 \cos(\alpha_0 + \theta + \delta) - \right. \\ & \left. 2g (L_1 \sin(\theta + \delta) + b \sin(\alpha_0)) \right] \end{aligned} \quad (10)$$

and:

$$\begin{cases} \frac{\partial L_{CR}}{\partial \dot{\alpha}_0} = m_n (b^2 \dot{\alpha}_0 + L_1 b \dot{\theta} \cos(\theta + \alpha_0 + \delta)) \\ \frac{d}{dt} \left(\frac{\partial L_{CR}}{\partial \dot{\alpha}_0} \right) = m_n \left[b^2 \ddot{\alpha}_0 + L_1 b \ddot{\theta} \cos(\theta + \alpha_0 + \delta) - \right. \\ \left. L_1 b \dot{\theta} (\dot{\theta} + \dot{\alpha}_0) \sin(\theta + \alpha_0 + \delta) \right] \\ \frac{\partial L_{CR}}{\partial \alpha_0} = -m_n (L_1 b \dot{\theta} \sin(\theta + \alpha_0 + \delta) + b g \cos(\alpha_0)) \end{cases} \quad (11)$$

The initial chair center rotation angle α_0 is controlled to change linearly according to the change in slope θ of the robot. The dynamic equation of the anti-overturn control mechanism on the robot stairs is established according to Lagrange is [17]:

$$\frac{d}{dt} \left(\frac{\partial L_{CR}}{\partial \dot{\alpha}_0} \right) - \frac{\partial L_{CR}}{\partial \alpha_0} = M_M \quad (12)$$

Substituting (11) into (12), the formula becomes:

$$M_M = m_n \begin{bmatrix} b^2 \ddot{\alpha}_0 + g b \cos(\alpha_0) + \\ L_1 b \left(\ddot{\theta} \cos(\theta + \alpha_0 + \delta) - \right. \\ \left. \dot{\theta}^2 \sin(\theta + \alpha_0 + \delta) \right) \end{bmatrix} \quad (13)$$

Considering the moment of resistance of the seat system affecting the seat rotation angle, we have the following equation:

$$M_M - f_r \dot{\alpha}_0 = m_n \left[\begin{array}{l} b^2 \ddot{\alpha}_0 + \\ L_1 b \left(\begin{array}{l} \ddot{\theta} \cos(\theta + \alpha_0 + \delta) - \\ \dot{\theta}^2 \sin(\theta + \alpha_0 + \delta) \end{array} \right) + \\ gb \cos(\alpha_0) \end{array} \right] \quad (14)$$

where f_r is the resistance moment coefficient of the chair, and M_M (N·m) is the moment generated from the electric cylinder.

B. Dynamic Equation of Anti-Overturn Mechanism at the End of the Stairs

Robots moving on stairs often overturn and lose balance at the last step of the stairs. The operation of the adaptive mechanism when moving to the last step will help the robot to be balanced, reduce oscillation, and reduce the phenomenon of overturning towards the stair platform. The location of the adaptive mechanism is placed on the robot as shown in Figure 1, the adaptive system is installed on the robot as shown in Figure 3, and the system coordinate system is set up as follows:

$$l_{xA} = L_{A2} \cos(\xi + \theta); \quad l_{yA} = L_{A2} \sin(\xi + \theta) \quad (15)$$

where l_{xA} and l_{yA} are the positions of the adaptive mechanism, L_{A2} (mm) is the distance between the passive wheel and the adaptive mechanism, v_{xA} , v_{yA} (m/s) is the velocity of the adaptive mechanism according to OX and OY, T_A (J), P_A (J) are the kinetic energy and potential energy of the adaptive mechanism, and M_A (N·m) is the moment of the adaptive mechanism. The kinetic energy equation of the system when in the state of preparing to move down the last step of the stairs is as follows:

$$\Sigma T_A = \frac{1}{2} m_e (v_{xA}^2 + v_{yA}^2) = \frac{1}{2} m_e L_{A2}^2 \dot{\theta}^2 \quad (16)$$

The potential energy of the anti-overturn system at the end of the stairs is as follows:

$$\Sigma P_A = m_e gh = m_e g L_{A2} \sin(\xi + \theta) \quad (17)$$

Then the system Lagrange equation will be:

$$L_A = \Sigma T_A - \Sigma P_A = \frac{1}{2} m_e (L_{A2}^2 \dot{\theta}^2 - 2g L_{A2} \sin(\xi + \theta)) \quad (18)$$

and:

$$\left\{ \begin{array}{l} \frac{\partial L_A}{\partial \dot{\theta}} = m_e L_{A2}^2 \dot{\theta} \\ \frac{d}{dt} \left(\frac{\partial L_A}{\partial \dot{\theta}} \right) = m_e L_{A2}^2 \ddot{\theta} \\ \frac{\partial L_A}{\partial \theta} = -m_e g \dot{\theta} L_{A2} \cos(\xi + \theta) \end{array} \right. \quad (19)$$

The dynamic equation of the anti-overturn mechanism at the end of the stairs of the human transport robot is constructed as follows:

$$M_A = \frac{d}{dt} \left(\frac{\partial L_A}{\partial \dot{\theta}} \right) - \frac{\partial L_A}{\partial \theta} \quad (20)$$

$$\Leftrightarrow M_A = m_e [L_{A2}^2 \ddot{\theta} + g \dot{\theta} L_{A2} \cos(\xi + \theta)]$$

In summary, the anti-roll control equation system for a robot transporting people up and down stairs will be:

$$\left\{ \begin{array}{l} M_M = m_n \left[\begin{array}{l} b^2 \ddot{\alpha}_0 + L_1 b \left(\begin{array}{l} \ddot{\theta} \cos(\theta + \alpha_0 + \delta) - \\ \dot{\theta}^2 \sin(\theta + \alpha_0 + \delta) \end{array} \right) + \\ gb \cos(\alpha_0) \end{array} \right] + f_r \dot{\alpha}_0 \\ M_A = m_e [L_{A2}^2 \ddot{\theta} + g \dot{\theta} L_{A2} \cos(\xi + \theta)] \end{array} \right. \quad (21)$$

IV. SIMULATION AND EXPERIMENT

A. Simulation Results

A simulation was conducted to verify the anti-overturn dynamic equations for the human transport robot on Matlab Simulink software. A sliding mode controller, with a sliding surface by PID equation (SMC-PID) [17] is used in the system control process. The simulation model is shown in Figure 4.

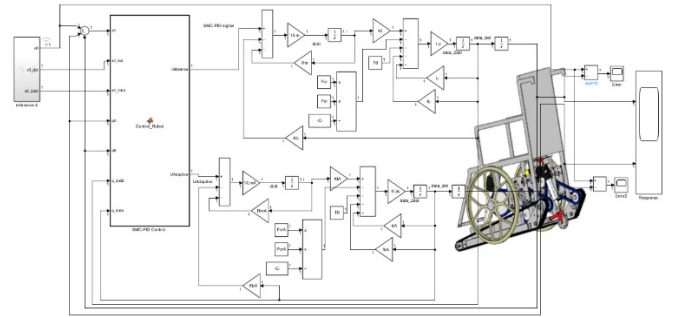


Fig. 4. Simulation model of the anti-overturn mechanism response for the robot.

Based on the built robot dynamics equation, the sliding control algorithm is built with the sliding surface in the form of a PID equation for the s_M balancing system and the s_A adaptive mechanism in the form:

$$s(t) = \dot{e}(t) + \lambda_1 e(t) + \lambda_2 \int e(t) dt \quad (22)$$

$$s_A(t) = \dot{e}_A(t) + r_1 e_A(t) + r_2 \int e_A(t) dt \quad (23)$$

where $e(t) = y(t) - x_0(t)$, $e_A(t) = y_A(t) - z_0(t)$ is the error between the output response and the desired signal, $y(t)$, $y_A(t)$ is the output signal, and $x_0(t)$, $z_0(t)$ is the desired signal. The coefficients λ_1 , r_1 , λ_2 , r_2 are chosen as positive coefficients so that the given meets the Hurwitz stability criterion, that is, it has its roots with negative real parts.

The Lyapunov stability criterion is used with a positive definite equation of the form:

$$T = \frac{1}{2} s^2 \tag{24}$$

Setup $x_{1A} = \theta$, $x_{2A} = \dot{\theta}$, $y_A = \theta = x_{1A}$, $u_A(t) = M_A$, and $x_1 = a_0$, $x_2 = a_0$, $y = a_0 = x_1$, $u(t) = M_M$.

The control law for the anti-rollover process is designed based on the PID equation slip surface:

$$\left\{ \begin{array}{l} u_M(t) = m_n \left(\begin{array}{l} L_1 b \dot{x}_{2A} \cos(x_{1A} + x_1 + \delta) - \\ L_1 b x_{2A}^2 \sin(x_{1A} + x_1 + \delta) + \\ g b \cos(x_1) + \\ \left[\begin{array}{l} \ddot{y}_0(t) - \lambda_1(x_2(t) - \dot{y}_0(t)) \\ -\lambda_2(x_1(t) - \dot{y}_0(t)) \\ -k \tanh(s_M(t)) \end{array} \right] \end{array} \right) + f_r x_2 \\ u_A(t) = m_e \left(\begin{array}{l} \left[\begin{array}{l} \ddot{z}_0(t) - r_1(x_{2A}(t) - \dot{z}_0(t)) \\ -r_2(x_{1A}(t) - z_{0A}(t)) \\ -k \tanh(s_A(t)) \end{array} \right] + \\ g x_{2A} L_{A2} \cos(\xi + x_{1A}) \end{array} \right) \end{array} \right. \tag{25}$$

The parameters of the anti-roll control system for the human transport robot and the sliding controller used in the simulation are presented in Table I.

TABLE I. ROBOT CONTROL SYSTEM SIMULATION PARAMETERS

Symbol	Legend	Value	Unit
m_R	Robot mass	50	kg
m_n	People mass (mass of matter)	100	kg
b	Distance from the center of gravity to the seat pivot	200	mm
L_1	Distance from the chair swivel joint to the driven wheel	700	mm
L_2	Distance from the adaptive mechanism to the driven wheel	800	mm
δ	The angle of elevation of the rotary joint relative to the driven wheel	15	(°)
F_{Cr}	Tilt angle	30-45	(°)
ξ	The angle of the adaptive mechanism	20	(°)
f_r	Friction coefficient	0.05	Nm
R_m, R_{mA}	The resistance of the electric cylinder	0.085	Ω
L_m, L_{mA}	The inductance of the electric cylinder	0.005	H
P_m	The screw lead	0.02	m
F_{Cr}	The output force of the electric cylinder	700	N
K	Positive constant	1.5	
η	The mechanical transmission efficiency	0.8	
λ_1, λ_2	Coefficients in the PID sliding surface	15; 290	
r_1, r_2	Coefficients in the PID sliding surface for the adaptive system	5; 190	

The simulation results for evaluating the robot's anti-overturn equation were conducted using a pulse input signal with amplitude 40 and a period of 20 s. The pulse function signal is presented in Figure 5. The tracking system responded

to the input with a system error of just 0.05 mm, and exhibited no overshoot. This makes the system able to balance the center of gravity of the seat, helping to prevent the robot from rolling. Figure 6 shows the experimental results with an arbitrary input signal (white noise).

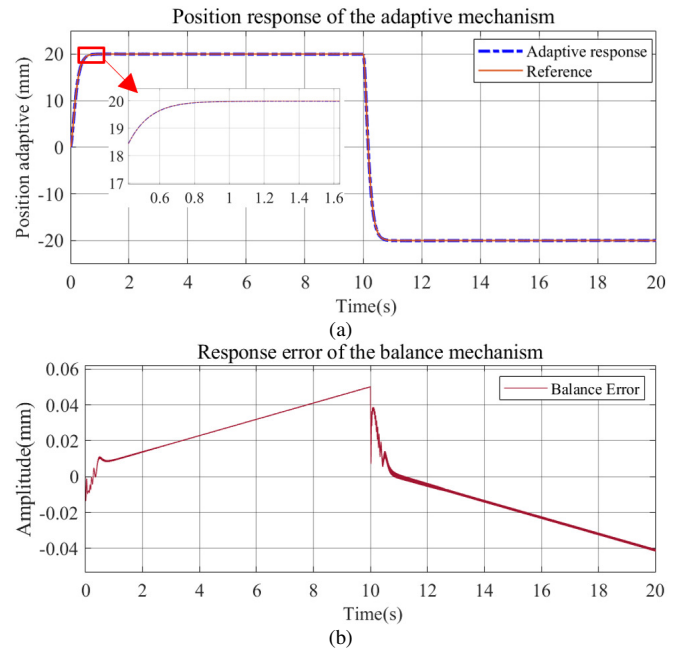


Fig. 5. Response and control error of the balancing mechanism of the human transport robot.

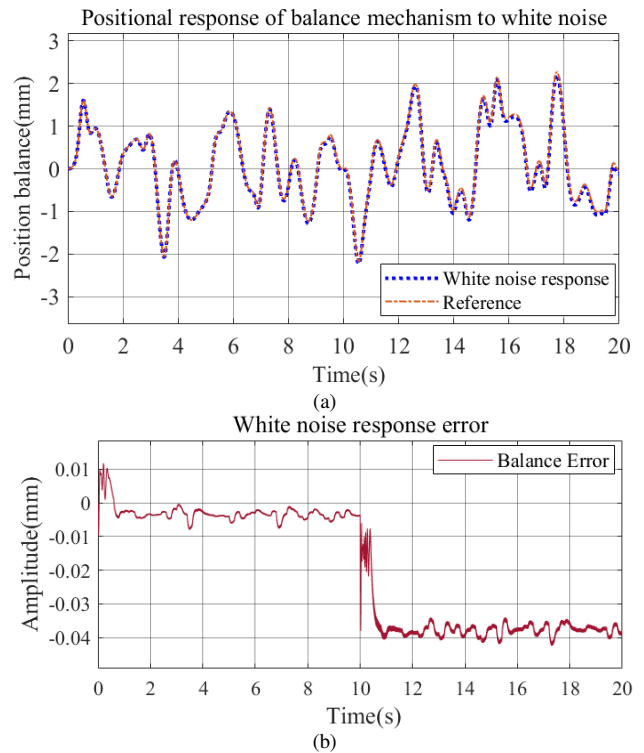


Fig. 6. White noise signal response and control error of the balancing mechanism of the human transport robot.

The simulation results with a white noise input signal with a noise power of 0.5, and a sampling time of 0.2 also give quite good results. The response of the balance system still follows the desired signal. The response error is not too large, fluctuating within 0.06 mm. Through simulation with types of input signals, pulse signal and white noise signal, the response error compared to the input is relatively small (0.05 - 0.06 mm), which can confirm the correctness of the dynamic equation of balance and anti-overturn when the robot moves on the stairs.

Similarly, the system simulates the anti-overturn model with the last step of the stairs. The simulation aims to test the adaptability of the actuator to the sudden change of the robot when moving up the last step of the stairs. The experimental input signal is a sine wave with amplitude $\pi/2$ and sample time period 10. The results, presented in Figure 7(a), show that the response of the actuator closely follows the desired sine wave signal, with a minimum response error of 0.0011 (Figure 7(b)).

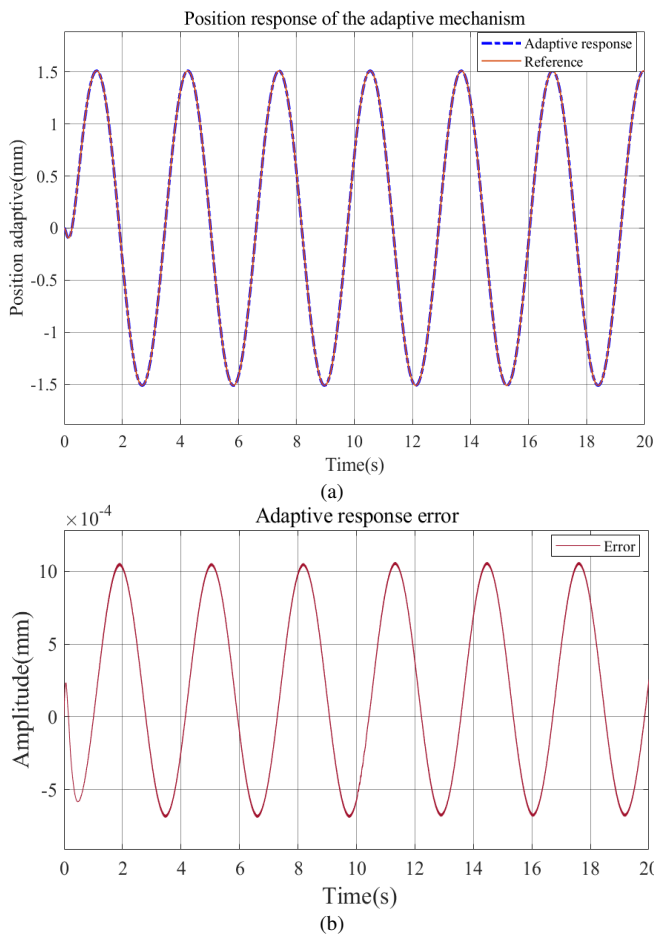


Fig. 7. Response and error of the anti-overturn mechanism at the last step of stairs using a sine wave.

Experiments with white noise signals have also yielded feasible results. The response follows the control signal and the error is 0.005 mm, as shown in Figure 8.

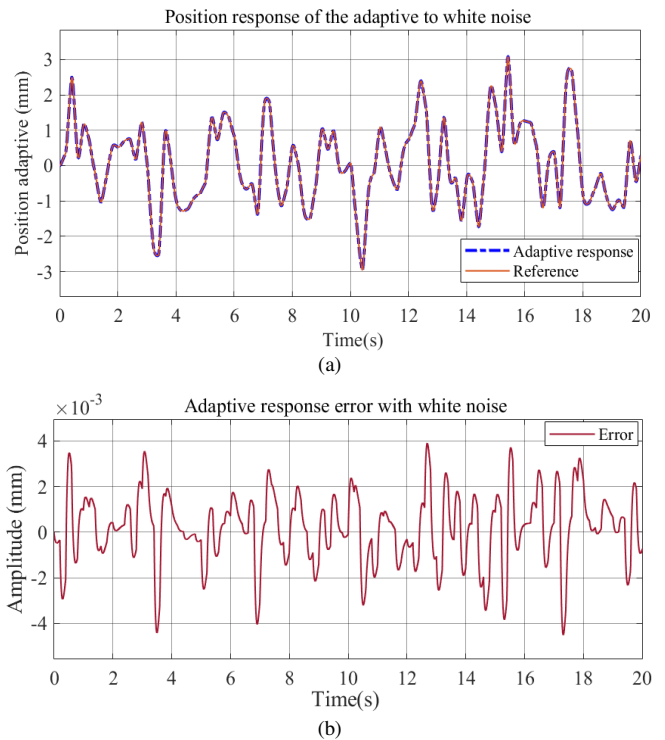


Fig. 8. Response and error of the anti-overturn mechanism at the last step of stairs using white noise.

The average deviation of the anti-roll system is relatively small, ranging from 0.0011 mm to 0.06 mm for the simulated signals. The amplitude of the output signals responds to the input signal types, but there are some fluctuations. Figure 9 illustrates the response test results for the balancing and adaptive mechanisms. The linear change between the two values of the anti-roll mechanism for the robot shows that the control process is feasible in the process of anti-roll and vibration reduction. Although the response is quite good, the response amplitude is different, which shows the delay in the system.

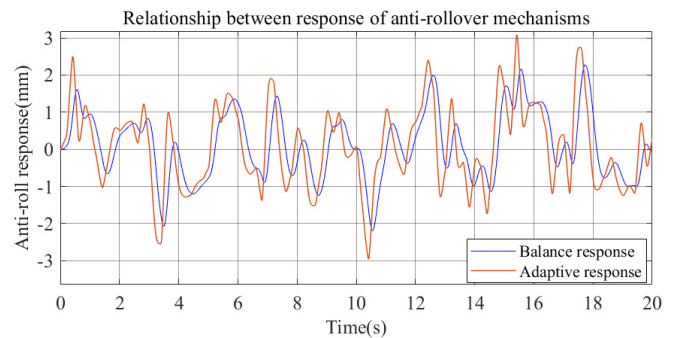


Fig. 9. Balanced and adaptive system relationships.

B. Experimental Control System for Anti-Overturning of Human Transport Robot

The actual experimental model uses the IMU 6050 sensor to determine the tilt angle for the robot, 02 E6B2-CWZ6C 2000

pulse/rev encoders mounted with the chair's rotating shaft to determine the movement of the anti-roll mechanism, 02 HY-SRF05 ultrasonic sensors are used to determine the distance and position of the robot when moving on the stairs, 01 E18-D80NK infrared sensor determines the status of the robot leaving the stairs, 01 Arduino mega 2560 circuit is used as the central circuit, 01 computer is used in the process of monitoring the control system signal, and the motors used in the system use power from a 12V-60AH battery. The system drive is specially designed with two modes: flat and on stairs. The experimental equipment requirements and setup locations are illustrated in Figure 10. The movement path of the anti-roll mechanism at the last step of the stairs is determined through a rotary encoder fixed to the rotating shaft of the electric cylinder fixing bar.

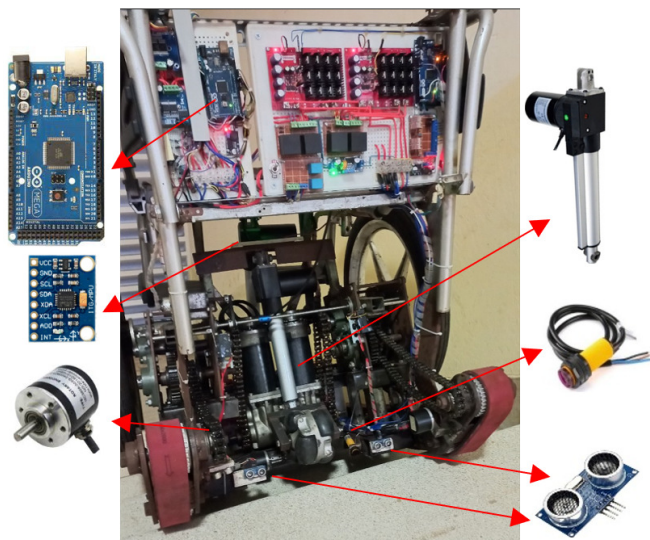


Fig. 10. Anti-rollover measurement and control system.

The experimental model employed to assess the anti-rollover control system for the robot is executed when the robot, bearing a load of 100 kg, traverses a staircase with a slope of 35°, a step width of 300 mm, a height of 150 mm, and a staircase width of 1200 mm. The experiment did not take into account the conditions for horizontal and vertical sliding. The evaluation process of the anti-overturn system is shown in Figure 11.

The experimental model was conducted using Matlab Simulink software. Figure 12(a) depicts the diagram of the anti-overturn control system on the stairs, whereas Figure 12(b) illustrates the diagram of the anti-overturn control at the last step of the stairs.

The Kalman filter is used in the signal processing process from the IMU sensor to the system. The balance system operates according to the change in tilt angle, controlling the robot's center of gravity to change according to the slope of the stairs. The experimental results were obtained through repeated trials in which the robot moved up and down stairs with the above dimensions. Experiments findings demonstrate that the response of the balance system follows the change in tilt angle,

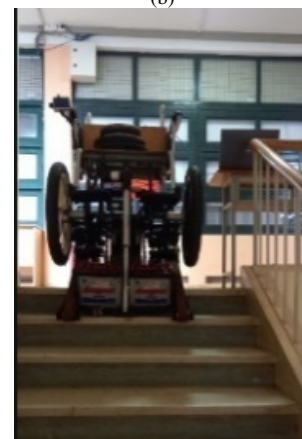
and the robot can still transport the mass of objects up and down the stairs stably and safely. The seat position is adjusted parallel to the ground so that the robot's center of gravity is balanced compared to the slope of the stairs. The anti-overturn ability through this control process is evaluated through the monitoring results using Matlab Simulink software on the computer. The results show that the response of the actuator is quite good according to the measured value from the IMU sensor, however, the response signal in the survey fluctuates, as shown in Figure 13(a). The robot moves along a trajectory characterized by a slope of 35°. The balance mechanism is stable, and the seat surface is parallel to the step surface at 32 s.



(a)



(b)



(c)

Fig. 11. Experimental setup and evaluation of the anti-overturn system in the human transport robot.

In the last step, the adaptive mechanism facilitates robot support through the established distance sensor signal. The measurement results are displayed in Figure 13(b), and the response of the balancing mechanism remains capable of following. The robot position follows the motion path of the adaptive mechanism; the large oscillation phenomenon is not seen in the measurement results, the oscillation is in the range of 2-3°, and the system still does not affect the overturning phenomenon.

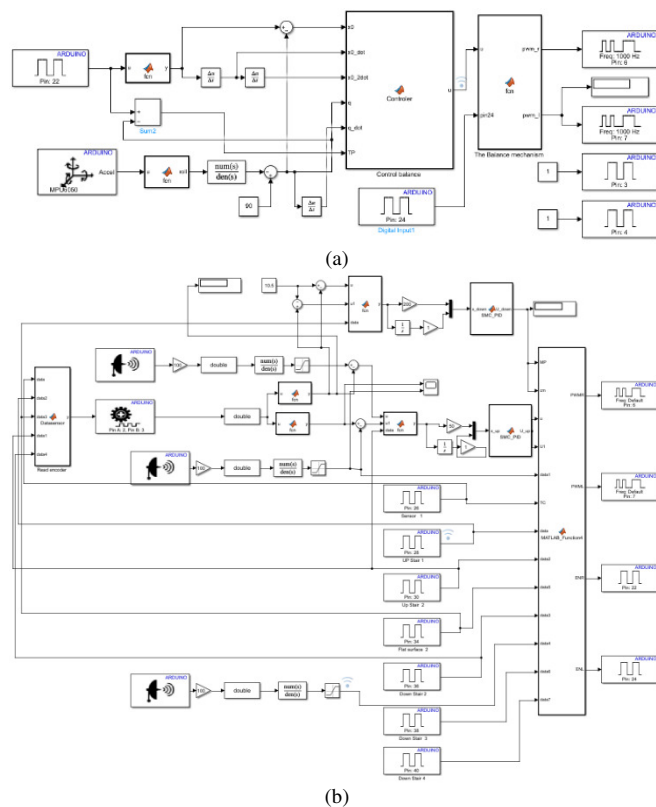
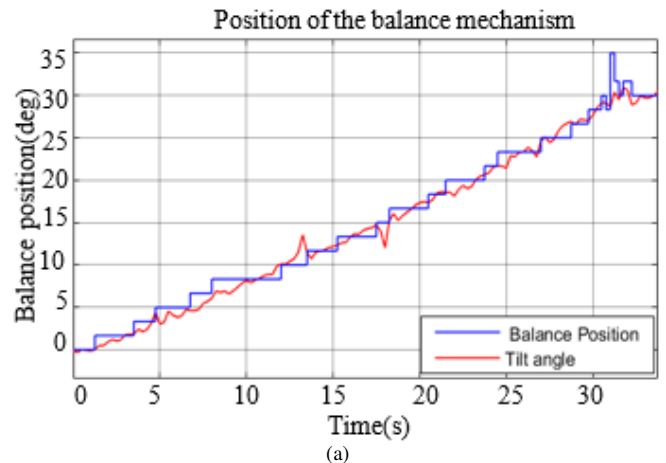
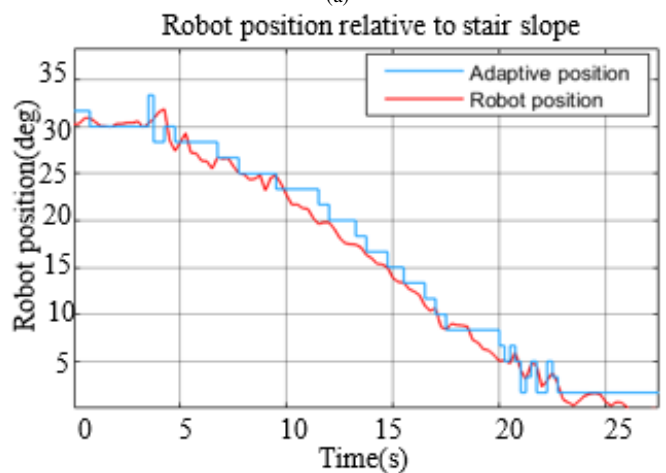


Fig. 12. Anti-overturn control model of the human transport robot: (a) anti-tip control when on stairs, and (b) anti-tip control at the end of the stairs.

The experiment of the robot moving down the stairs starts with the measurement system that determines the position of the robot at the top of the stairs. The adaptive system performs the process of adapting to the slope of the stairs when moving down the stairs through the sensor value that measures the distance of the stairs to the crawler. The results show that the anti-overturn system on the stairs follows the change in the robot's tilt, as shown in Figure 14. After 18 s, the robot reaches the position it needs to move down. The robot starts moving down at 24 s, the anti-roll mechanism at the end of the stairs begins to retract, the robot's center of gravity is also lowered, and the balance system still follows this change. The results show that the signal and response of the anti-roll system do not have large fluctuations, so the operation of the anti-roll mechanism at the end of the stairs and the robot's balance mechanism have limited the oscillation and the phenomenon of overturning.



(a)



(b)

Fig. 13. Robot-balanced response when moving up and down stairs.

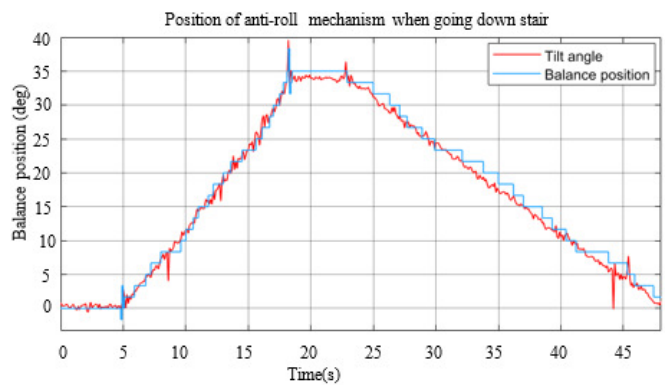


Fig. 14. Anti-tip response when going downstairs.

The experiments show that the response of the robot system is stable to the changing factors during the robot's movement. The system has an adaptive response to the system moving on the stairs, the IMU sensor signal determines the robot position and is processed by the Kalman estimation algorithm, contributing to the accuracy of the control system. The experimental results in Figure 14 show that the response follows the measurement signal, however, during the time of moving down, the sensor signal and the actuator response have

many deviations. Starting from 25 s, the robot system moves down with the sensor signal linear to the slope of the stairs, and the balance mechanism response, although adaptive, has a large deviation of about 3°. This deviation is due to the influence of the hardware and some interference factors from the measuring device. The research results of applying the SMC-PID control algorithm based on the construction of the dynamic equation of the robot moving up and down the stairs have many advantages over the research [8]. The control process is stable with environmental control, the error is smaller than the study using the PID algorithm (error 4°, experimental slope 30°), and there is no automatic anti-roll system [14].

V. CONCLUSION

The anti-roll control equation system for the robot transporting people up and down the stairs of the building at the last step and on the stairs is established based on the robot structure and the Lagrange theory. The robot balance control is achieved through the regulation of the seat position relative to the flat surface. The anti-roll control when the robot changes state at the last step of the stairs is implemented through the automatic adaptation mechanism. The simulation results demonstrate that the center of gravity position of the robot follows the reference value, the error approaches zero, and there is no overshoot. The response of the balance system still follows the desired signal, with a response error that fluctuates within 0.06 mm. Thus, it can be substantiated that the equation for robot balance dynamics is accurate. Furthermore, the experimental results demonstrate that the robot can safely transport people up and down stairs at a slope of 35°. The actuator response still follows the measurement signal from the sensor, the oscillation phenomenon within the system is not too large (3°), and the up-and-down movement of the robot ensures that the anti-overturn system adjusts according to the measurement value. Compared with the previous experimental results [21], the anti-overturn system at the end of the stairs provides better efficiency, and the oscillation phenomenon is reduced.

In this study, a balancing and adaptive system is designed to prevent tipping and reduce vibration for the robot with a higher level of automation than previous studies such as those cited in [7] and [10]. The actuator response, controlled by the SMC-PID algorithm, enhances the robot's anti-tipping capability when navigating stairs. Compared with the PID control algorithm in the studies [13] and [16], the experimental response when the robot carried the load exhibited a fairly good response with a tilt angle of the stair, as demonstrated in Figures 13 and 14. In contrast, the tilt angle response of the study in [16] exhibits a greater deviation of approximately 4°.

The study has effectively implemented the anti-overturning process for the robot when moving up and down stairs. The control of the robot's center of gravity through the regulation of the seat balance as a counterweight assists in mitigating the overturning phenomenon resulting from the deviation of the center of gravity according to the slope. Furthermore, the adaptive mechanism control process is implemented to limit the oscillation phenomenon at the bottom step of the stairs. In the future, the research team will continue to develop intelligent controllers based on the anti-rollover dynamic

equations of human transport robots. The refinement of the intelligent trajectory motion control [22] and the influencing factors will be carried out shortly.

ACKNOWLEDGMENT

The research team sincerely thanks the leaders of Vinh Long University of Technical Education and all lecturers of the Faculty of Mechanical Engineering for supporting and creating conditions for the research team to complete this research goal.

REFERENCES

- [1] V.-T. Nguyen and T. T. Tung, "Design and Development of a Wheelchair Prototype," *Engineering, Technology & Applied Science Research*, vol. 14, no. 2, pp. 13376–13379, Apr. 2024, <https://doi.org/10.48084/etasr.6851>.
- [2] A. Pappalettera, F. Bottiglione, G. Mantriota, and G. Reina, "Watch the Next Step: A Comprehensive Survey of Stair-Climbing Vehicles," *Robotics*, vol. 12, no. 3, Jun. 2023, Art. no. 74, <https://doi.org/10.3390/robotics12030074>.
- [3] T. Seo, S. Ryu, J. H. Won, Y. Kim, and H. S. Kim, "Stair-Climbing Robots: A Review on Mechanism, Sensing, and Performance Evaluation," *IEEE Access*, vol. 11, pp. 60539–60561, 2023, <https://doi.org/10.1109/ACCESS.2023.3286871>.
- [4] X. Gao, D. Cui, W. Guo, Y. Mu, and B. Li, "Dynamics and stability analysis on stairs climbing of wheel-track mobile robot," *International Journal of Advanced Robotic Systems*, vol. 14, no. 4, Jul. 2017, Art. no. 1729881417720783, <https://doi.org/10.1177/1729881417720783>.
- [5] S. S. P. K. Reddy, C. S. Teja, K. Susmitha, and D. H. Rao, "Design and Analysis of stair climbing wheelchair," *International Research Journal of Engineering and Technology*, vol. 8, no. 2, pp. 154–161, Feb. 2021.
- [6] W. Tao, Y. Ou, and H. Feng, "Research on Dynamics and Stability in the Stairs-Climbing of a Tracked Mobile Robot," *International Journal of Advanced Robotic Systems*, vol. 9, no. 4, Oct. 2012, Art. no. 146, <https://doi.org/10.5772/52850>.
- [7] W. Tao, Y. Jia, T. Liu, J. Yi, H. Wang, and Y. Inoue, "A novel wheel-track hybrid electric powered wheelchair for stairs climbing," *Journal of Advanced Mechanical Design, Systems, and Manufacturing*, vol. 10, no. 4, Aug. 2016, Art. no. JAMDMS0060, <https://doi.org/10.1299/jamdsm.2016jamdsm0060>.
- [8] H. Rastan, "Mechanical Design for Track Robot Climbing Stairs," M.S. thesis, University of Ottawa, Ottawa, Canada, 2011.
- [9] L. Jing-yi, B. Yang, J. Fei, W. Dong-xiao, and G. Xue-shan, "Mechanics analysis of a wheelchair robot with wheel-track coupling mechanism," *Journal of Beijing Institute of Technology*, vol. 22, no. 3, pp. 301–307, 2013.
- [10] B. Sharma, B. M. Pillai, K. Borvorntanajanya, and J. Suthakorn, "Modeling and Design of a Stair Climbing Wheelchair with Pose Estimation and Adjustment," *Journal of Intelligent & Robotic Systems*, vol. 106, no. 3, Nov. 2022, Art. no. 66, <https://doi.org/10.1007/s10846-022-01765-3>.
- [11] G. Quaglia, M. Nisi, W. Franco, and L. Bruzzone, "Dynamic Simulation of an Electric Stair-Climbing Wheelchair," *International Journal of Automation Technology*, vol. 11, no. 3, pp. 472–480, May 2017, <https://doi.org/10.20965/ijat.2017.p0472>.
- [12] T.-C. Jiang, S.-H. Yin, and E. Tanaka, "Wheelchair Able to Assist the Elderly to Move on Stairs and Stand up," in *2019 58th Annual Conference of the Society of Instrument and Control Engineers of Japan*, Hiroshima, Japan, 2019, pp. 1168–1173, <https://doi.org/10.23919/SICE.2019.8859944>.
- [13] A. A. Jorge, L. A. M. Riascos, and P. E. Miyagi, "Modelling and Controlling of a Hybrid Motorized Wheelchair on Flat and Inclined Surfaces," in *2019 6th International Conference on Control, Decision and Information Technologies*, Paris, France, 2019, pp. 750–755, <https://doi.org/10.1109/CoDIT.2019.8820679>.
- [14] S. R. Thamel, R. Munasinghe, and T. Lalitharatne, "Motion Planning of Novel Stair-Climbing Wheelchair for Elderly and Disabled People," in

- 2020 Moratuwa Engineering Research Conference, Moratuwa, Sri Lanka, 2020, pp. 590–595, <https://doi.org/10.1109/MERCon50084.2020.9185273>.
- [15] G. Quaglia, W. Franco, and M. Nisi, "Evolution of Wheelchair, a Stair-climbing Wheelchair," in *Proceedings of the 14th IFToMM World Congress*, Taipei, Taiwan, 2015, pp. 135–144, <https://doi.org/10.6567/IFToMM.14TH.WC.OS13.032>.
- [16] M. F. Ilma Suryanto, N. Alim Badriawan, E. S. Ningrum, E. Henfri Binugroho, and N. F. Satria, "Balance Control on the Development of Electric Wheelchair Prototype with Standing and Stair Climbing Ability with Tracked-Wheel Mechanism," in *2018 International Electronics Symposium on Engineering Technology and Applications*, Bali, Indonesia, 2018, pp. 43–47, <https://doi.org/10.1109/ELECSYM.2018.8615523>.
- [17] H. Medjoubi, A. Yassine, and H. Abdelouahab, "Design and Study of an Adaptive Fuzzy Logic-Based Controller for Wheeled Mobile Robots Implemented in the Leader-Follower Formation Approach," *Engineering, Technology & Applied Science Research*, vol. 11, no. 2, pp. 6935–6942, Apr. 2021, <https://doi.org/10.48084/etasr.3950>.
- [18] N. Zerroug, K. Behih, Z. Bouchama, and K. Zehar, "Robust Adaptive Fuzzy Control of Nonlinear Systems," *Engineering, Technology & Applied Science Research*, vol. 12, no. 2, pp. 8328–8334, Apr. 2022, <https://doi.org/10.48084/etasr.4781>.
- [19] D. T. Dat, T. D. Thuan, and L. H. Ky, "Application of SMC-PID algorithm for anti-roll control for human-carrying robot," *Journal of Military Science and Technology*, vol. 100, pp. 128–138, Dec. 2024, <https://doi.org/10.54939/1859-1043.j.mst.100.2024.128-138>.
- [20] D. Morin, *Introduction to Classical Mechanics: With Problems and Solutions*. Cambridge, UK: Cambridge University Press, 2008, <https://doi.org/10.1017/CBO9780511808951>.
- [21] D. T. Dat, L. H. Ky, V. Duong, and D. V. Chia, "Control Solutions for Stair Climbing Robot Mechanism," *Journal of Harbin Engineering University*, vol. 45, no. 10, pp. 131–137, Oct. 2024.
- [22] T. T. K. Ly, N. T. Thanh, H. Thien, and T. Nguyen, "A Neural Network Controller Design for the Mecanum Wheel Mobile Robot," *Engineering, Technology & Applied Science Research*, vol. 13, no. 2, pp. 10541–10547, Apr. 2023, <https://doi.org/10.48084/etasr.5761>.